Chaos in nuclei: Theory and experiment

IOP Conf. Series: Journal of Physics: Conf. Series **1023** (2018) 012011 doi:10.1088/1742-6596/1023/1/012011

Chaos in nuclei: Theory and experiment

L. Muñoz[1], R. A. Molina[2], J. M. G. Gómez[1]

[1] Grupo de Física Nuclear, Facultad de Ciencias Físicas, Universidad Complutense, E-28040 Madrid, Spain

[2] Instituto de Estructura de la Materia, IEM-CSIC, Serrano 123, Madrid, E-28006, Spain

E-mail: jmgomezg@ucm.es

Abstract.

During the last three decades the quest for chaos in nuclei has been quite intensive, both with theoretical calculations using nuclear models and with detailed analyses of experimental data. In this paper we outline the concept and characteristics of quantum chaos in two different approaches, the random matrix theory fluctuations and the time series fluctuations. Then we discuss the theoretical and experimental evidence of chaos in nuclei. Theoretical calculations, especially shell-model calculations, have shown a strongly chaotic behavior of bound states in regions of high level density. The analysis of experimental data has shown a strongly chaotic behavior of nuclear resonances just above the one-nucleon emission threshold. For bound states, combining experimental data of a large number of nuclei, a tendency towards chaotic motion is observed in spherical nuclei, while deformed nuclei exhibit a more regular behavior associated to the collective motion. On the other hand, it had never been possible to observe chaos in the experimental bound energy levels of any single nucleus. However, the complete experimental spectrum of the first 151 states up to excitation energies of 6.20 MeV in the ^{208}Pb nucleus have been recently identified and the analysis of its spectral fluctuations clearly shows the existence of chaotic motion.

1. Introduction

The atomic nucleus is generally considered a paradigmatic case of quantum chaos. Intuitively one can expect that fast moving nucleons interacting with the strong nuclear force and bound in the small nuclear volume should give rise to a chaotic motion. During the last three decades the quest for chaos in nuclei has been quite intensive, both with theoretical calculations using nuclear models and with detailed analyses of experimental data. Statistical spectroscopy studies in nuclei have been also motivated by a desire to understand the implications of chaotic behavior in many-body quantum systems [1].

In this paper we outline the concept and characteristics of quantum chaos in two different approaches, the Random Matrix Theory (RMT) fluctuations [2] and the time series fluctuations [3]. Although these two approaches are conceptually different, they lead to the same conclusions, namely, that both chaotic and regular quantum systems exhibit a universal but different behavior in the statistical properties of the spectrum. Furthermore it has been proven that, when the fluctuations of random matrix ensembles are studied with methods from time series analysis, all the ensembles exhibit $1/f$ noise, independently of the system symmetries [4].

Then we discuss the theoretical and experimental evidence of chaos in nuclei. Theoretical calculations, especially shell-model calculations, have shown a strongly chaotic behavior of bound

states at higher excitation energy, in regions of high level density [5]. In the low energy region most shell-model calculations show chaotic behavior as well, however, there are exceptions, for example, in neutron-rich Ca and Pb isotopes [6, 7]. The analysis of experimental data has shown a strongly chaotic behavior of nuclear resonances just above the one-nucleon emission threshold [8]. For bound states, combining experimental data of a large number of nuclei, a tendency towards chaotic motion is observed in spherical nuclei, while deformed nuclei exhibit a more regular behavior. For a comprehensive review of chaos in nuclei see for example Gómez *et al.* [1] and Weidenmüller and Mitchell [9]. On the other hand, it had never been possible to observe chaos in the experimental bound states of any single nucleus. However, very recently the complete experimental spectrum of 151 states up to excitation energies of 6.20 MeV in the ^{208}Pb nucleus have been identified at the Maier-Leibnitz-Laboratorium at Garching, Germany [10], and the analysis of its spectral fluctuations clearly shows the existence of chaotic motion in the nuclear bound states of ^{208}Pb [11, 12].

2. Quantum chaos and spectral fluctuations

2.1. Random Matrix Theory and quantum chaos

The concept of chaos in classical mechanics is well established, but the criteria that characterize classical chaos, like exponential divergence of trajectories, cannot be carried to quantum mechanics. From the study of quantum billiards with chaotic classical analogues, Bohigas, Giannoni and Schmidt (BGS) reached the following conjecture: the spectral fluctuation properties of simple quantum systems known to be ergodic in the classical limit, are universal and follow very closely those of the Gaussian ensembles of random matrices [2]. The BGS conjecture has been proven in the semiclassical limit [13]. The essential feature of chaotic energy spectra in quantum systems is the existence of level repulsion and correlations. On the contrary, classically integrable systems give rise to uncorrelated adjacent energy levels, that are well described by Poisson statistics [14].

The most commonly used statistics to characterize spectral fluctuations are the nearest neighbor spacing (NNS) distribution $P(s)$ and the spectral rigidity $\Delta_3(L)$ of Dyson and Mehta [15]. For the sequence of unfolded levels $\epsilon_i, i = 1, ..., N$, the nearest level spacing s_i is defined by $s_i = \epsilon_{i+1} - \epsilon_i$ and the average values are $\langle s \rangle = 1$, $\langle \epsilon_n \rangle = n$.

For the uncorrelated levels or Poisson case, $P_P(s) = \exp(-s)$, $P_P(0) = 1$, and $\langle \Delta_3(L) \rangle = L/15$. For the Gaussian orthogonal ensemble (GOE), $P(s)$ follows very closely the Wigner surmise $P_W(s) = (\pi/2)s \exp(-\pi s^2/4)$ and the $\langle \Delta_3(L) \rangle$ grows logarithmically instead of linearly.

2.2. Time series approach to quantum chaos

One of the main tools in the study of time series fluctuations is the power spectrum of the signal. For many different phenomena in nature, physics and social sciences, the power spectrum of a signal is characterized by a power law. To study correlations in the fluctuations of quantum spectra, we can consider the energy spectrum as a discrete signal, and the sequence of energy levels as a time series, where the level order index plays the role of a discrete time [3]. The power spectrum $S(k)$ of a discrete spectrum with $N + 1$ levels is calculated as

$$\delta_n = \sum_{i=1}^{n} (s_i - \langle s \rangle), \quad \hat{\delta}_k = \frac{1}{N} \sum_n \delta_n \exp\left(\frac{-2\pi i k n}{N}\right), \quad S(k) = \left|\hat{\delta}_k\right|^2. \tag{1}$$

The study of quantum billiards, nuclei and random matrices, suggested the following conjecture: the energy spectra of chaotic quantum systems are characterized by $1/f$ noise, while the energy spectra of regular quantum systems are characterized by $1/f^2$ noise [3]. This conjecture relates chaotic quantum systems with other complex systems in nature that are also characterized by $1/f$ noise [16].

3. Quantum chaos in nuclei

3.1. Chaos in experimental energy spectra

For a quantum system like the atomic nucleus, which has no classical limit, the term chaos started to be used when Haq, Pandey and Bohigas [8] analyzed the spectral fluctuations of experimental neutron and proton $J^\pi = 1/2^+$ resonances just above the one-nucleon emission threshold and showed that they agree very well with those of the Gaussian Orthogonal Ensemble (GOE) of Random Matrix Theory (RMT). Thus, in this sense, it is clear that nuclei are very chaotic in the energy region just above the one-nucleon emission threshold.

But for bound states, the situation is not so clear, because a good analysis of fluctuations in experimental energy spectra requires the knowledge of sufficiently long, pure and complete sequences, i.e. with the same $J^\pi T$ values and without missing levels or $J^\pi T$ misassignments. But this ideal situation is rarely found in nuclei. For very light nuclei the number of bound levels is not sufficient for statistical purposes. For medium and heavy nuclei the identified levels are limited to the ground state region, because at higher energy the level density becomes very high and the experimental identification of J^π values becomes generally impossible. In order to improve statistics, Shriner *et al.* combined level spacings from different nuclei into a single set to analyze the behavior of the $P(s)$ distribution [17]. Separating the data in six different mass regions a clear trend from GOE to Poisson is observed as the nuclear mass increases. Generally spherical nuclei are closer to GOE and deformed nuclei are closer to Poisson.

3.2. Chaos in shell-model calculations

In order to get a deeper understanding of what happens in the low-energy region we can use the shell model with configuration mixing. Realistic shell-model calculations in *sd* shell nuclei show a strong chaotic behavior [5]. As an illustrative example of the RMT approach, Fig. 1 shows the shell-model $P(s)$ and $\langle\Delta_3(L)\rangle$ values for the $J^\pi = 2^+,\ T = 0$ states of ^{28}Si obtained by Zelevinski *et al.* [5]. Clearly the agreement with GOE is excellent. As an example of the time series approach, Fig. 2 shows the $1/f$ noise behavior in the average power spectrum of a combination of sequences of states with different values of J^π in ^{34}Na and ^{24}Mg.

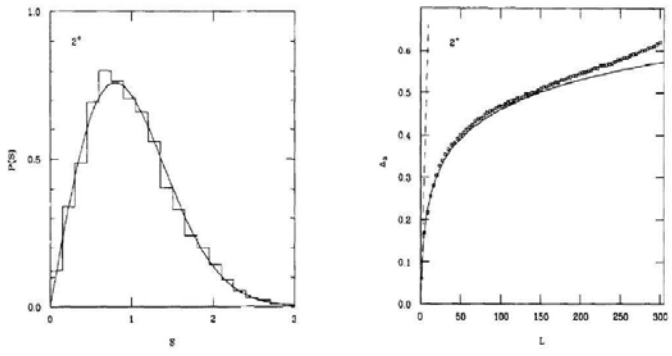

Figure 1. Spectral statistics for the $J^\pi = 2^+,\ T = 0$ states of ^{28}Si. *Left panel* $P(s)$ distribution. *Right panel* $\langle\Delta_3(L)\rangle$ [5].

In *pf* shell nuclei the dimensionalities of the shell-model valence space are much larger than in the *sd* shell and it becomes possible to study with realistic shell-model calculations how chaos depends on isospin and excitation energy [6]. In nuclei with both protons and neutrons in the valence space, the shell-model results show spectral fluctuations close to GOE. However, when all valence particles are neutrons, the spectral fluctuations deviate from chaotic behavior. These results can be interpreted in terms of the strength of the nuclear residual interaction. The mean

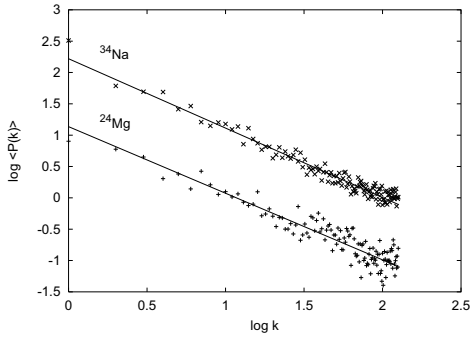

Figure 2. Average power spectrum of levels of the nuclei ^{34}Na and ^{24}Mg [3].

field generates regular motion and the residual interaction produces strong correlations that lead to chaotic motion. But, since the nn residual interaction is much weaker than the pn interaction, valence neutrons only may not be enough to strongly perturb the regular mean-field motion. Fig. 3 shows the isospin dependence of $\langle\Delta_3(L)\rangle$ for $J^\pi = 0^+$, $T = T_z$ levels in $A = 46$ isobars. In ^{46}Ca, there are only valence neutrons and $\langle\Delta_3(L)\rangle$ quickly deviates from the GOE curve for $L > 8$. In ^{46}Sc there are one proton and five neutrons outside the core and the chaotic behavior is very clear up to $L \approx 26$. In ^{46}Ti, the number of pn interactions is larger and there are no significant deviations from GOE.

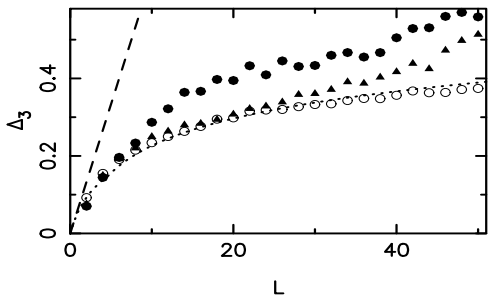

Figure 3. $\langle\Delta_3(L)\rangle$ for $J^\pi = 0^+$, $T = T_z$ levels in $A = 46$ isobars, ^{46}Ca (full dots), ^{46}Sc (triangles), ^{46}Ti (empty dots). The dotted and dashed curves represent the GOE and Poisson values, respectively [6].

3.3. Spectral statistics in the experimental ^{208}Pb bound states.
Experimental nuclear spectra become increasingly plagued with unidentified states, missing levels and some misassignments as excitation energy increases. But we consider that the recent accurate data on ^{208}Pb [10] enable a meaningful statistical analysis of level fluctuations in a nucleus, with pure, complete, and reasonably long sequences.

Fluctuations are the departure of the actual level density from a local uniform density. Therefore it is essential to eliminate the smooth part of the exponential increase of the nuclear density, mapping the actual spectrum onto a quasiuniform spectrum with mean spacing $\langle s\rangle = 1$. This step, called unfolding, is delicate and of utmost importance, because some of the unfolding procedures used in the literature can lead to completely wrong results on the behavior of level fluctuations [18]. In this work we have used the constant temperature formula [17]. A separate unfolding has been performed for all J^π sequences with a minimum of 5 known consecutive

states. The longest sequence corresponds to the $J^\pi = 3^-$ states, with 19 consecutive levels. Gathering the unfolded spacings for all J^π into a single set, there are 115 spacings.

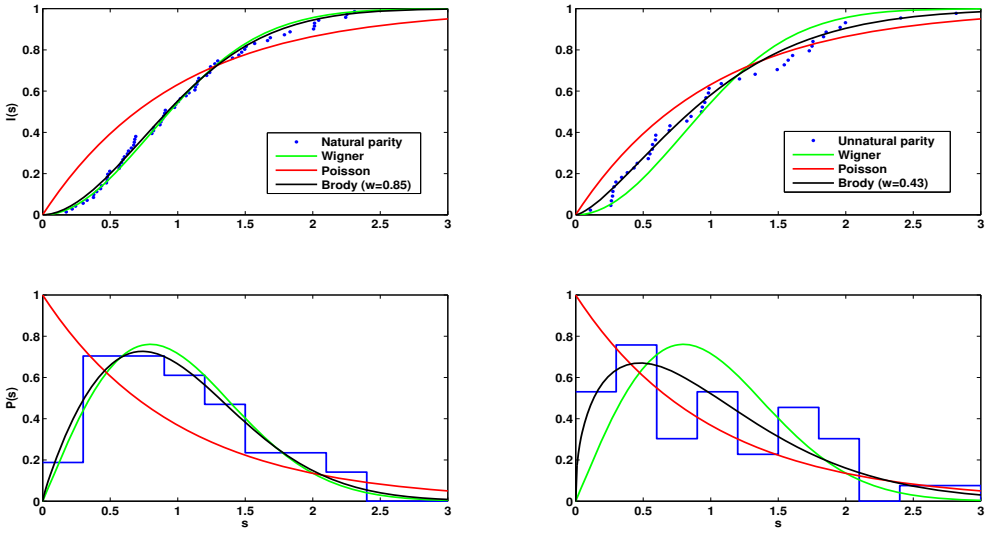

Figure 4. Comparison of spectral fluctuation statistics for natural parity states (left panels) and unnatural parity states (right panels) in ^{208}Pb. Panels (a) and (b) show the cumulative nearest neighbor spacing (cumulative NNS) distribution for experimental levels (dots). Panels (c) and (d) show the NNS distribution $P(s)$ for experimental levels (histogram). In all panels the green (light gray) line is the Wigner surmise, the red dashed line is the Poisson distribution, and the black solid line is the best fit Brody distribution.

A simple way to interpolate between the Poisson limit $P_P(s)$ and the Wigner surmise $P_W(s)$ is provided by the Brody distribution,

$$P_B(s,\omega) = (\omega+1)a_\omega s^\omega \exp(-a_\omega s^{\omega+1}), \quad a_\omega = \left[\Gamma\left(\frac{\omega+2}{\omega+1}\right)\right]^{\omega+1}, \tag{2}$$

where Γ is the gamma function. The Brody parameter ω is given by the best fit to the histogram of $P(s)$. When the number of spacings is not very large, the $P(s)$ distribution may depend on the choice of histogram binning size. It is then preferable to fit the cumulative distribution $I(s) = \int_0^s dx P(x)$. For the full set of 115 spacings the best Brody fit to the experimental $I(s)$ is obtained for $\omega = 0.68$. This value is certainly much closer to the Wigner limit ($\omega = 1$) than to the Poisson limit ($\omega = 0$) but it is still rather far from full chaotic behavior.

3.4. Comparison of short-range spectral fluctuations in natural and unnatural parity states
Heusler *et al.* have shown [10] that the experimental unnatural parity levels in ^{208}Pb ($J^\pi = 0^-, 1^+, 2^-, \ldots, 11^+$) agree better than the natural parity states ($J^\pi = 0^+, 1^-, 2^+, \ldots, 12^+$) with the so-called "extended schematic shell model", which is a simplified shell-model consisting mainly of 1p-1h mean-field configurations . The excitation energies of 70 states with unnatural parity agree within about 0.2 MeV with the extended schematic shell model. By contrast, the excitation energies of about 20 natural parity states are more than 0.5 MeV lower than the model prediction. They conclude theerefore that the residual interaction is much stronger for natural than for unnatural parity states.

Table 1. Number of spacings, Brody parameter ω and rms deviation from Wigner and Poisson distributions for different parity sets in the experimental states of ^{208}Pb at $E_x < 6.20$ MeV.

Parity	all	natural	unnatural
Number of spacings	115	71	44
Brody ω	0.68	0.85	0.43
$(\text{RMSD})_W$	0.040	0.025	0.077
$(\text{RMSD})_P$	0.115	0.129	0.088

To check if this effect can be observed in the fluctuation measures, we have analyzed separately the NNS distribution of experimental natural and unnatural parity states. Table 1 shows the number of unfolded spacings of each type at $E_x < 6.20$ MeV in ^{208}Pb and the corresponding values of the Brody parameter obtained from the fit of the cumulative distribution, as well as the root mean square deviation (RMSD) of the experimental $I(s)$ from the Wigner and Poisson limits. Fig. 4 shows the distributions $I(s)$ and $P(s)$ for natural and unnatural parity states, compared to Wigner, Poisson and the best fit of the Brody distribution.

For natural parity states the behavior is definitely chaotic, with $\omega = 0.85$. The Brody and Wigner curves for $P(s)$ nearly coincide, and the dots representing the cumulative distribution clearly follow the Wigner distribution. To our knowledge, this is the closest GOE behavior ever observed in experimental nuclear bound states. It is worth to comment that the Wigner surmise is only a good analytical approximation to the GOE distribution, and that the best fit of $P_B(s,\omega)$ to the exact $P(s)$ distribution for GOE is obtained for $\omega = 0.957$, not for $\omega = 1$ [19].

By contrast, for unnatural parity states the cumulative distribution is intermediate between the two extremes, somewhat closer to Poisson, with $\omega = 0.43$. There are only 44 spacings and the histogram of $P(s)$ oscillates a lot. But notice especially the different behavior of $P(s)$ for small spacings in natural and unnatural parity states. Level repulsion is seen to be much stronger for natural parity states. Strong level repulsion is characteristic of chaotic (Wigner-like) spectra, whereas for the regular motion $P(s)$ is maximal for small spacings.

We should keep in mind that the experimental J^π sequences in nuclei are generally quite short and that any missing levels or misassignments always bias the statistical measures towards Poisson. In the case of ^{208}Pb all the states with $E_x < 6.20$ MeV are now well identified and we are confident that the NNS distribution is not biased by missing levels or misassignments. The results reflect the degree of chaos caused by the residual interaction, and this is clearly seen comparing the NNS distributions of natural and unnatural parity states.

4. Conclusions

Many shell-model calculations of bound states in spherical nuclei have clearly shown the existence of chaotic dynamics produced by the strong residual NN interaction which destroys the mean-field regular motion. The study of spectral fluctuations in experimental bound states is generally limited by the short length of $J^\pi T$ sequences, uncertainties in some quantum number assignments and possible missing levels. Nevertheless, combining data from many different nuclei along the nuclear chart, a clear trend from GOE to Poisson is observed as the nuclear mass increases. However, a fully chaotic spectrum has never been observed in these kind of analysis. This fact can be understood because at lower excitation energies many states are dominated by a few shell-model configurations. On the other hand, generally spherical nuclei are closer to GOE and deformed nuclei are closer to Poisson. This makes sense because the lower energy spectrum of deformed nuclei comes mainly from collective rotational motion, which is a regular motion.

The recent identification with spin and parity assignment of all the 151 states at $E_x < 6.20$

MeV in ^{208}Pb by Heusler *et al.* [10] has provided exceptionally long J^π sequences of consecutive states free of missing levels and misassignments, enabling us to perform a reliable analysis of spectral fluctuations in this nucleus. Comparison of the experimental spectrum with extended 1p-1h schematic shell-model calculations clearly indicate that the residual interaction is much stronger for natural than for unnatural parity states [10]. A recent analysis of spectral fluctuations has shown [11] that natural parity states exhibit results close to GOE and the unnatural parity states are far from GOE behavior. Thus these results indicate that chaotic and non-chaotic states coexist in the energy region from the ground state up to 6.20 MeV excitation energy (the neutron threshold in ^{208}Pb is $S_{\rm n} = 7.368$ MeV). Furthermore, our analysis of the experimental spectrum has confirmed, to our knowledge for the first time, a well-known shell-model prediction, namely that chaos in nuclei arises when the residual interaction is strong enough to destroy the ordered motion of nucleons in the nuclear mean field.

Finally, let us point out that another analysis of spectral fluctuations of the same experimental states of ^{208}Pb has been published [12]. They use two chaoticity measures different from ours and do not observe a significant difference between experimental natural and unnatural parity states. Possibly this difference with our results is due to the different unfolding procedures used. The influence of the unfolding method can be important for such a small number of levels as the unnatural parity states of ^{208}Pb. On the other hand, the spectral fluctuations have been analyzed by the same authors for two different shell-model calculations in ^{208}Pb. It should be noticed that the shell-model J^π sequences are much larger than the experimental ones and therefore the unfolding procedure is more reliable. The shell-model values of the chaoticity parameters are different for natural and unnatural parity, the natural parity states being more chaotic, in agreement with our results.

5. Acknowledgment

This research was conducted with support of MINECO/FEDER Grant Nos. FIS2015-63770-P and FPA2015-65035-P.

References

[1] J.M.G. Gómez, K. Kar, V.K.B. Kota, R.A. Molina, A. Relaño, and J. Retamosa, Phys. Rep. **499**, 103 (2011).
[2] O. Bohigas, M.J. Giannoni, C. Schmit, Phys. Rev. Lett. **52**, 1 (1984).
[3] A. Relaño, J.M.G. Gómez, R.A. Molina, J. Retamosa, E. Faleiro, Phys. Rev. Lett. **89**, 244102 (2002).
[4] E. Faleiro, J.M.G. Gómez, R.A. Molina, L. Muñoz, A. Relaño, J. Retamosa, Phys. Rev. Lett. **93**, 244101 (2004).
[5] V. Zelevinsky, B.A. Brown, N. Frazier, M. Horoi, Phys. Rep. **276**, 85 (1996).
[6] R.A. Molina, J.M.G. Gómez, J. Retamosa, Phys. Rev. C **63**, 014311 (2000).
[7] R.A. Molina, Eur. Phys. J. A **28**, 125 (2006).
[8] R.U. Haq, A. Pandey, O. Bohigas, Phys. Rev. Lett. **48**, 1086 (1982).
[9] H.A. Weidenmüller, G.E. Mitchell, Rev. Mod. Phys. **81**, 539 (2009).
[10] A. Heusler, R. V. Jolos, T. Faestermann, R. Hertenberger, H.-F. Wirth, and P. von Brentano, Phys. Rev. C **93**, 054321 (2016).
[11] L. Muñoz, R.A. Molina, J.M.G. Gómez, A. Heusler, Phys. Rev. C **95** , 014317 (2017).
[12] B. Dietz, A. Heusler, K.H. maier, A. Richter, B.A. Brown, Phys. Rev. Lett. **118**, 012501 (2017).
[13] S. Müller, S. Heusler, P. Braun, F. Haake, A. Altland, Phys. Rev. Lett. **93**, 014103 (2004).
[14] M.V. Berry, M. Tabor, Proc. R. Soc. Lond. **A 356**, 375 (1977).
[15] F.J. Dyson, M.L. Mehta, J. Math. Phys. **4**, 701 (1963).
[16] L.M Ward, P.E. Greenwood, Scholarpedia **2**, 1537 (2007).
[17] J.F. Shriner Jr., G.E. Mitchell, T. von Egidy, Z. Phys. A − Hadrons and Nuclei **338**, 309 (1991).
[18] J.M.G. Gómez, R.A. Molina, A. Relaño, J. Retamosa, Phys. Rev. E **66**, 03
[19] T.A. Brody, J. Flores, J.B. French, P.A. Mello, A. Pandey, S.S.M. Wong, Rev. Modern Phys. **53**, 385 (1981).